



MATHEMATICAL SIMULATION OF UNSTEADY FLOW THROUGH HOLLOW FIBER MEMBRANE

Riyadh Zuhair Al Zubaidy, Ph. D.

Raghad Samir Mahmood, M. Sc.

Department of Water Resources Engineering, University of Baghdad

ABSTRACT

Water flowing through hollow fiber membrane comprises two types of flow each having its own hydraulic characteristics. The first is the flow inside the fiber channel, and the second is the flow through the fiber porous wall. Water flow through hollow fiber membrane, HFM, is unsteady nonuniform flow due to the accumulation of rejected material on the fiber surface causing a change in the hydraulic resistance along the fiber length with time. Under these conditions, a mathematical model was developed to simulate water flow through hollow fiber membrane based upon the equations governing the flow inside the fiber channel and through the fiber wall, equations governing conditions imposed by flow boundaries, and implicit finite difference technique for solving partial differential equations. The model was verified by using published laboratory experimental data. A very good agreement was obtained between the measured and predicted flowrate values under the same conditions.

The mathematical model was applied to three types of commercially available fiber modules to investigate variation of flux, the transmembrane pressure, the thickness of the rejected materials along the fiber length, the flowrate, and the effect of the pot length on the fiber hydraulic performance. It was found there is considerable variation in the hydraulic performance of the three types of fiber. Therefore, the mathematical model provides a tool to work on finding the optimal design of the hollow fiber membrane.

الخلاصة

ان جريان الماء في الاغشية الليفية المجوفة يتضمن نوعين من الجريان لكل منهما خواصة الهيدروليكية، الاول جريان الماء داخل قناة الليف والثاني جريان الماء خلال جداره النفاذ. ان جريان الماء في الاوعية الليفية هو جريان غير ثابت وغير منتظم لتتغير المقاومة الهيدروليكية على امتداد الليف مع الزمن نتيجة تراكم الترسبات على سطح الليف. تحت هذه الظروف تم اعداد نموذج رياضي لمحاكاة جريان الماء خلال الليف بالاعتماد على المعادلات التي تحكم الجريان داخل قناته وخلال الجدار النفاذ له والمعادلات التي تحكم الجريان عند حدود الجريان. تم التحقق من اداء النموذج الرياضي باستخدام قياسات مختبرية منشورة ووجد بان هنالك توافق جيد بين هذه القيم والقيم المستحصلة من النموذج.

استخدم النموذج في تحري تغير التدفق والضغط عبر غشاء الليف وسمك الترسبات على امتداد الليف والتصريف الكلي واثراطول المحكم من الليف لثلاثة انواع من الالياف المجوفة التجارية. وجد بان هنالك تفاوت كبير في الاداء الهيدروليكي للانواع الثلاث من الالياف. لذا فان النموذج الرياضي المعد يوفر الاداة للعمل على ايجاد التصميم الامثل للالياف المجوفة.

KEYWORDS

Hollow fiber membrane, mathematical model, microfiltration.

INTRODUCTION

Membranes technology represents an important new set of processes for drinking water treatment. Hollow fiber membrane modules become one of the most popular membrane modules used in industry and water treatment. Hollow fiber membrane modules are used in a variety of membrane filtration processes. They typically consist of many fibers arranged in parallel as a bundle in a shell tube and sealed with potting material at each end. Filtration can occur from the outside of the fiber to the inside, or vice versa. Filtration in membrane processes occurs as a result of driving force acting on the feed water.

Water flowing through hollow fiber membrane comprises two types of flow each having its own hydraulic characteristics. The first is the flow inside the fiber channel, and the second is the flow through the fiber wall.

The main objectives of this paper are to develop and verify a mathematical model to simulate the unsteady flow through the hollow fiber membrane module, based on the equations governing the flow inside the fiber channel, and Darcy's formula, which is governing the flow through the fiber wall, and to examine the hydraulic performance of some existing hollow fiber membrane modules.

MATHEMATICAL MODEL

The mathematical simulation of unsteady flow through the hollow fiber membrane during actual operation was developed based on the equations governing the flow through the fiber wall and the fiber channel as described in the following sections.

Equations Governing Flow inside Hollow Fiber Membrane Channel

Flow of water inside hollow fiber membrane channel may be classified as one dimensional unsteady nonuniform flow. **Fig. 1** is a schematic longitudinal section along a flow segment through hollow fiber membrane.

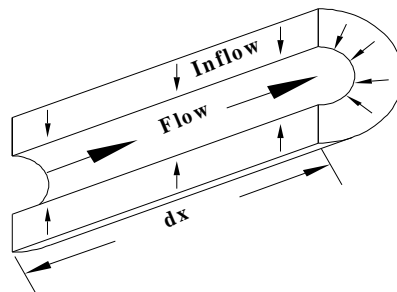


Fig. 1. A schematic longitudinal section along a fiber segment.

The equations governing such a flow are obtained by applying two physical principles, namely conservation of mass and conservation of momentum, to the flow segment. The resulting



equations are two quasi-linear partial differential equations. The derivation of these equations can be found in reference such as, Chaudhary, 1986. These equations can be written as:

$$\frac{\partial H}{\partial t} + \frac{Q}{A} \frac{\partial H}{\partial x} - \frac{Q}{A} \sin \alpha + \frac{a^2}{gA} \frac{\partial Q}{\partial x} - \frac{a^2}{gA} q_w = 0 \tag{1}$$

and

$$\frac{\partial Q}{\partial t} + \frac{Q}{A} \frac{\partial Q}{\partial x} + gA \frac{\partial H}{\partial x} + \frac{fQ|Q|}{2idA} + \frac{Q}{A} q_w = 0 \tag{2}$$

In which

H = piezometric head, (L),

Q = flowrate, (L³/T),

a = speed of the pressure wave, (L/T),

A = cross sectional area of fiber channel, (L²),

x = horizontal distance along fiber, (L),

t = time, (T),

α = angle of the fiber inclination with the horizontal coordinate,

q_w = flux, lateral inflow rate per unit length of fiber, (L³/T/L),

f = friction factor, (dimensionless),

id = inner diameter of the fiber, (L), and

g = gravitational acceleration, (L/T²).

In eqs. (1) and (2), there are two independent variables, x and t , three dependent variables, Q , H and q_w . Other variables, A and id , are characteristics of the fiber system and are time-invariant. Friction factor is assumed to vary with the Reynolds number, R_e , and is evaluated depending upon the flow type. The pressure wave speed in fiber is calculated according to fiber and water properties. Assuming no gas bubbles or fluid vapor appear, the wave speed is considered not to change during the unsteady state.

Equations Governing Flow through Fiber Wall and Rejected Material Layer

The flow of water through the fiber wall is a one dimensional unsteady flow. Darcy's law can be used to estimate the flowrate through the fiber wall and the rejected material layer. The following simplified assumptions are usually made in the model:

1. The medium forming the fiber wall is symmetric, i.e., it has a constant hydraulic conductivity,
2. The average size of the particle accumulation on the outer fiber surface is larger than the pore size of the fiber, i.e., the membrane hydraulic conductivity does not change with time,
3. The rejected material layer is incompressible; the porosity and hydraulic conductivity are independent of the applied feed pressure,
4. The rejected material layer is homogenous and has same hydraulic conductivity along the length of the fiber,
5. The rejected material layer is uniform porous structure, and
6. The applied feed pressure is constant along the fiber and does not change with time.

The flow of water through a fiber segment of a unit length is governed by Darcy's Law and can be written in polar coordinate system as, Al Zubaidy, 2007:

$$q_w = 2\pi K_w \frac{(H_o - H)}{\ln\left(\frac{r_o}{r_i}\right)} = 2\pi K_w \frac{TMP}{\ln\left(\frac{r_o}{r_i}\right)} \tag{3}$$

In which

K_w = hydraulic conductivity of the fiber wall, (L/T),
 TMP = Transmembrane pressure head, (H_o-H), (L),
 H = the head inside the fiber channel, (L),
 H_o = the head outside the fiber, the applied head, (L),
 r_o = the fiber outer radius, (L), and
 r_i = the fiber inner radius, (L).

The hydraulic conductivity, K_w , is a measure of the ability of water to flow through a fiber wall. It depends on the fluid and the fiber properties. During actual filtration process, the rejected materials starts to accumulate on the fiber wall and over all K_w starts to vary with time. **Fig. (2)** shows a schematic cross section through a fiber wall and the rejected material layer; an equivalent layer can be substituted for the fiber wall and the rejected material layer. The radial flowrate is the same for the fiber wall and rejected material layer, the total TMP is equal to the sum of TMP of the fiber wall and the rejected material layer, that is:

$$TMP_{equivalent\ layer} = TMP_{fiber\ wall} + TMP_{rejected\ material\ layer} \quad (4)$$

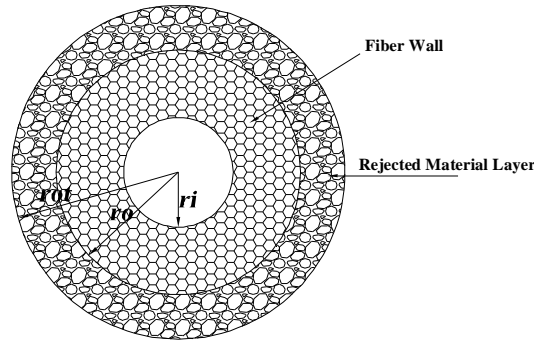


Fig. (2). A schematic cross section through a fiber wall and rejected material layer.

Substituting an expression for TMP from **eq. (3)**, **eq. (4)** may be written as:

$$\frac{q_w \ln\left(\frac{r_{ot}}{r_i}\right)}{2\pi K_{eq}} = \frac{q_w \ln\left(\frac{r_o}{r_i}\right)}{2\pi K_w} + \frac{q_w \ln\left(\frac{r_{ot}}{r_o}\right)}{2\pi K_c} \quad (5)$$

In which

r_{ot} = the rejected material layer outer radius, (L),
 K_c = the rejected material hydraulic conductivity, (L/T), and
 K_{eq} = equivalent hydraulic conductivity, (L/T).

Rearranging eq. (5), an expression for an equivalent hydraulic conductivity may be written as:

$$K_{eq} = \frac{\ln\left(\frac{r_{ot}}{r_i}\right)}{\frac{\ln\left(\frac{r_o}{r_i}\right)}{K_w} + \frac{\ln\left(\frac{r_{ot}}{r_o}\right)}{K_c}} \tag{6}$$

Eq. (3) may be written now as:

$$q_w = 2pK_{eq} \frac{TMP}{\ln\left(\frac{r_{ot}}{r_i}\right)} \tag{7}$$

The *TMP* in the above equation refers to the equivalent *TMP* of the rejected materials and the fiber wall.

The rejected material layer outer radius is changing during the filtration process as the rejected materials accumulated on the fiber surface. The variation of the rejected material layer outer radius is mainly affected by particle concentration in the raw water, *C*, rejected material density, ρ_c , flux, and the filtration time increment, Δt . An expression for obtaining the new outer radius of the rejected material layer after Δt of filtration was derived and is given by the expression:

$$r_{ot}^{new} = \sqrt{r_{ot}^{old} + \frac{C \Delta t q_w}{p r_c}} \tag{8}$$

SOLUTION PROCEDURE

The equations governing the unsteady flow state conditions in a hollow fiber membrane, eqs. (1) and (2), are two quasi-linear, hyperbolic, partial differential equations. The numerical simulation of the equations of unsteady flow described as follows: consider a nonuniform rectangular grid on the x-t plane as shown in Fig. (3). The distances along the fiber are represented by abscissas and ordinates represent times. Each point is identified by a subscript *i* which designates the x-position and a superscript *j* for the time line. The t-axis, where x=0, may be used as the upstream fiber boundary location, and the last line drawn parallel to the t-axis, to be designated the nth line, can be used to represent the downstream boundary location.

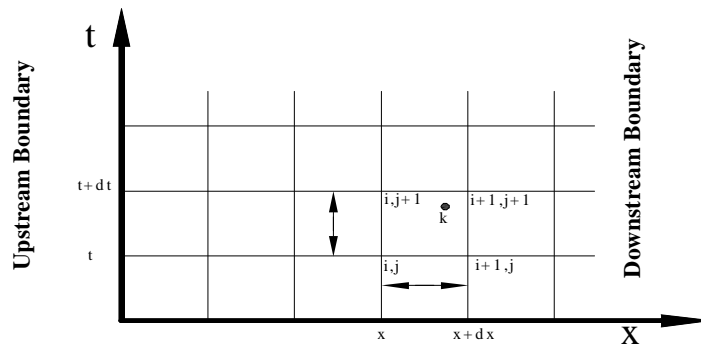


Fig. (3). Network of points on x, t-plane.

The space and time derivatives of a function $F(x, t)$ in the intervals *i, i+1* and *j, j+1* can be expressed as:

$$\frac{\partial F}{\partial x} = \frac{\theta(F_{i+1}^{j+1} - F_i^{j+1}) + (1-\theta)(F_{i+1}^j - F_i^j)}{\Delta x} \quad (9)$$

and

$$\frac{\partial F}{\partial t} = \frac{F_{i+1}^{j+1} + F_i^{j+1} - F_{i+1}^j - F_i^j}{2\Delta t} \quad (10)$$

In addition, the value of $F(x, t)$ can be approximated by:

$$F = \frac{\theta(F_{i+1}^{j+1} + F_i^{j+1}) + (1-\theta)(F_{i+1}^j + F_i^j)}{2} \quad (11)$$

The weighing factor θ is given a value between 0.5 and 1.0. A value $\theta=0.5$ is known as the "box" scheme, which is used in this study, while $\theta=1$ is the fully implicit scheme.

Applying the approximation concepts given by eqs. (9) to (11) to the derivative and non-derivative terms in the unsteady flow, eqs. (1) and (2), the finite difference formulations of the continuity, C_i , and momentum, M_i , equations for node i becomes

$$\begin{aligned} M_i = & \frac{1}{2\Delta t} [Q_{i+1}^{j+1} + Q_i^{j+1} - Q_{i+1}^j - Q_i^j] + \frac{1}{2A\Delta x} [q(Q_{i+1}^{j+1} + Q_i^{j+1}) + (1-q)(Q_{i+1}^j + Q_i^j)] \\ & * [q(Q_{i+1}^{j+1} - Q_i^{j+1}) + (1-q)(Q_{i+1}^j - Q_i^j)] + \frac{gA}{\Delta x} [q(H_{i+1}^{j+1} - H_i^{j+1}) + (1-q)(H_{i+1}^j - H_i^j)] \\ & + \frac{1}{4idA} [q(f_{i+1}^{j+1} Q_{i+1}^{j+1} |Q_{i+1}^{j+1}| + f_i^{j+1} Q_i^{j+1} |Q_i^{j+1}|) + (1-q)(f_{i+1}^j Q_{i+1}^j |Q_{i+1}^j| + f_i^j Q_i^j |Q_i^j|)] \\ & + \frac{1}{4A} [q(Q_{i+1}^{j+1} + Q_i^{j+1}) + (1-q)(Q_{i+1}^j + Q_i^j)] * [q(q_{wi+1}^{j+1} + q_{wi}^{j+1}) + (1-q)(q_{wi+1}^j + q_{wi}^j)] = 0 \end{aligned} \quad (12)$$

and

$$\begin{aligned} C_i = & \frac{1}{2\Delta t} [H_{i+1}^{j+1} + H_i^{j+1} - H_{i+1}^j - H_i^j] + \frac{1}{2A\Delta x} [q(Q_{i+1}^{j+1} + Q_i^{j+1}) + (1-q)(Q_{i+1}^j + Q_i^j)] \\ & * [q(H_{i+1}^{j+1} - H_i^{j+1}) + (1-q)(H_{i+1}^j - H_i^j)] - \frac{\sin a}{2A} [q(Q_{i+1}^{j+1} + Q_i^{j+1}) + (1-q)(Q_{i+1}^j + Q_i^j)] \\ & + \frac{a^2}{gA\Delta x} [q(Q_{i+1}^{j+1} - Q_i^{j+1}) + (1-q)(Q_{i+1}^j - Q_i^j)] - \frac{a^2}{2gA} [q(q_{wi+1}^{j+1} + q_{wi}^{j+1}) + (1-q)(q_{wi+1}^j + q_{wi}^j)] = 0 \end{aligned} \quad (13)$$

Where:

$$q_{wi+1}^{j+1} = 2pK_{eq_{i+1}}^{j+1} \frac{(TMP_{i+1}^{j+1})}{\ln\left(\frac{r_{ol_{i+1}}^{j+1}}{r_i}\right)} \quad (14)$$

Fig. (4) shows a schematic diagram of a fiber membrane insulated in an actual fiber module. The pot distance, L_{pot} is required to seal the fibers by using a special sealant so that all the flowrate of the module will be through the fiber wall and through the fiber channels along the effective length of the fiber, L_{total} . The fiber has two outlets at both ends, which means the flow of the fiber membrane module is symmetrical. Therefore, the flowrate calculations will be carried out on one half and for the whole flow for the fiber is twice the calculated. In this paper, the appropriate length for use in the model is half of the effective length that is L . The length, L is divided into $n-1$ segments each has a length of Δx . Usually, the node numbering starts from the upstream end down to the downstream end, e.g., node number 1 and number n refer to the nodes at the upstream and downstream, respectively. Node number 1 is at the half of the effective length of the fiber, node number n is at the open end.

In eqs. (12) and (13) all the terms associated with the j^{th} time line are known either from the initial conditions or from previous computations. This system of nonlinear equations cannot be solved directly since these four unknowns, H and Q at points i and $i+1$ on the $j+1$ time line, and only two equations. However, if similar equations are formed for each of the $n-1$ segments between upstream and downstream boundaries, a total of $2N-2$ equations with $2N$ unknowns are obtained. Two auxiliary equations are needed to make the number of equations equal to the number of unknowns which is obtained by the upstream and downstream boundary conditions. The systems of nonlinear equations are solved by Newton-Raphson's iterative method.

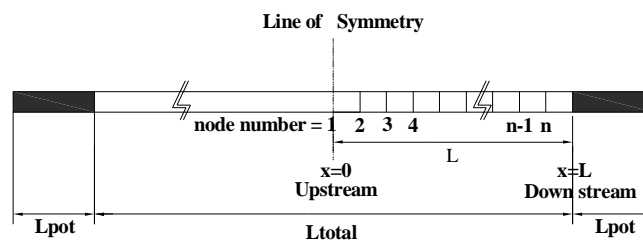


Fig. (4). A schematic diagram of a fiber membrane.

At the upstream boundary, $x=0$, the flowrate is equal to zero. At the downstream boundary, $x=L$, the pressure is constant and is equal to atmospheric pressure. When considering the pot as a part of the fiber, the equations governing the flow conditions through the pot channel are similar to the equations governing the flow through the fiber length except the last terms of eqs. (1) and (2), representing the effects of lateral flow, are ignored.

In order to start the computations of flow, initial flow conditions are required. The initial conditions can be obtained from computation of previous modeling process or it may be assumed arbitrarily then adjusted by operation of unsteady state model with pure water. The solution will converge rapidly, after few iterations in the first and second time steps and the correct results are produced regardless of the values of the assumed initial conditions.

MATHEMATICAL MODEL VERIFICATION

The developed mathematical model was calibrated and verified by using published laboratory experimental data to check the performance of the model and the validity of the assumptions made. Laboratory experiments, presented by Al-Zubaidy, 2007, were selected for verification, and were carried out on polypropylene, with inner and outer diameters of $0.39mm$ and $0.65mm$, respectively. The fibers were divided into four sets each set consists of ten fibers. The flowrate, under a constant head of $2m$, of each set was measured with its initial length, and then the flowrate is measured each once after reducing the length of the fibers.

The data of the first set were used for calibrating the hydraulic conductivity of the membrane with its initial length. It was found that the hydraulic conductivity coefficient of the measuring sets is equal to $4.64 \times 10^{-9} m/sec$ and it gives a minimum sum of squares of relative errors between predicted and measured flowrate.

For purpose of mathematical model operation, a distance increment of $1cm$, weighing factor, θ , of 0.55 , and a calculation tolerance limit of 0.0001 for both head and flowrate were used during the runs. The mathematical model was used then to predict the flowrate values of the fibers sets by just changing the fibers length. **Fig. (5)** shows a comparison between measured and mathematical model predicted flowrate values for different lengths. A good agreement between the measured and predicted flowrates values can be seen with a correlation coefficient value of 0.99 .

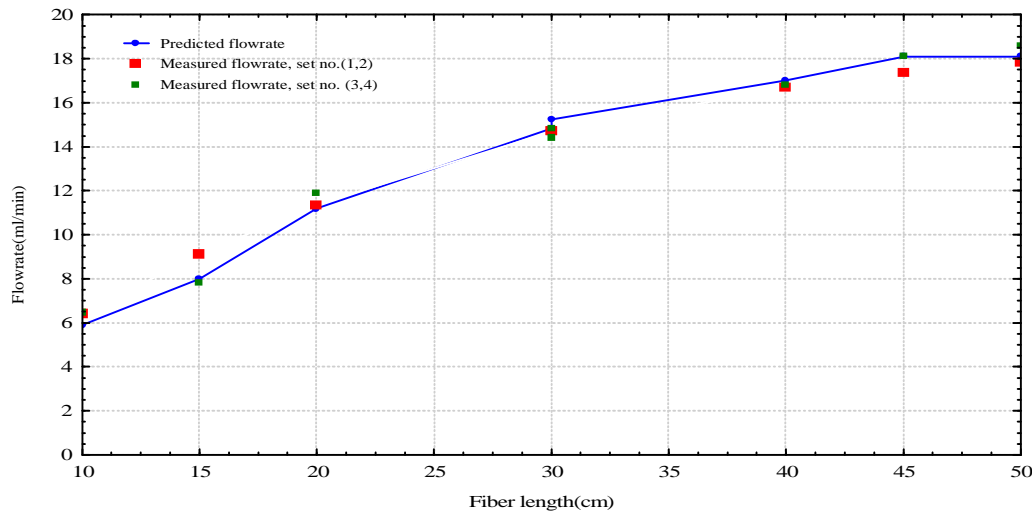


Fig. (5). Comparison between measured and predicted flowrate of fibers with different lengths.

APPLICATION OF THE UNSTEADY FLOW MATHEMATICAL MODEL

The developed mathematical model being calibrated and verified was used to study the hydraulic performance of the hollow fiber membrane. It was applied to investigate the hydraulic performance of three selected existing commercial hollow fiber membrane modules having different specifications under the conditions: the hollow fiber membrane is horizontal, the applied head is $2m$, and the hydraulic performance was studied in half of the effective length of the fiber.

Fouling analysis was performed assuming the water to be treated containing $0.25mg/l$ of clay. The hydraulic conductivity coefficient of the clay is $10^{-8}m/sec$ and the specific gravity of the clay is 1.49 , Singh and Punmia, 1970.

First Hollow Fiber Membrane Module

The specifications of the first type hollow fiber membrane modules that were hydraulically analyzed using the developed mathematical model are listed in **Table (1)**.

Table (1). Specifications of the third hollow fiber membrane module.

Parameter	Value
Fiber inner diameter, <i>mm</i> .	0.25
Fiber outer diameter, <i>mm</i> .	0.55
Number of fibers per module.	20 000
Effective fiber length, <i>cm</i> .	97
Pot length, <i>cm</i> .	10
Hydraulic conductivity coefficient of membrane, <i>m/sec</i> .	2.32×10^{-8}

Figs. (6) through (10) show the variation of the flux, transmembrane pressure head, thickness of rejected material layer along the fiber length with time, total fiber flowrate, and the effect of the pot on the ends of the fiber on the total flowrate.. Initially, the flux is nonuniform distributed along the fiber; the flux is very high near the exit end of the fiber. The flux drops by 99.8% between the two ends of the fiber as a result of the TMP reduction due to high head loss through the fiber's channel. About 80% of the total flowrate is within the 1st 10cm. The nonuniform flux distribution along the fiber leads to a nonuniform distribution of the rejected material along the fiber. A great reduction in the flux accrued within the 8hrs of filtration, at the exit the flux is reduced to 33% of its initial value. The total fiber flowrate is reduced about 50% of its initial flowrate after 24hr of filtration. The flowrate tends to be high during the initial time, after several hours, it declines off dramatically, the flowrate at open end decline, which was defined as $(initial\ flowrate - final\ flowrate) / initial\ flowrate$, is about 38.4% during the first eight hours. Then the flowrate at open end continues to decline, but at a much slower rate, the flowrate at open end declines to 8.6%, and 5% for the second, and last eight hours, respectively. It was found when using a pot at the end of the hollow fiber membrane; the flowrate at open end is reduced because of a very high head loss through the pot length but difference decreases with the time as the flowrate decreases. Initially the decrease is 58%, dropping to 43.2%, 41%, and 39.8% at $t=8, 16, 24hrs$, respectively.

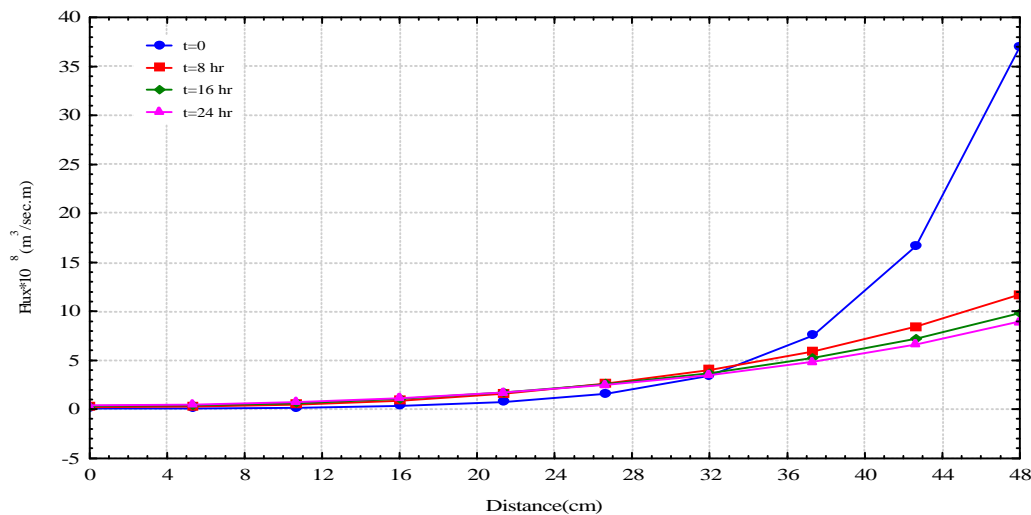


Fig. (6). Flux variation along the fiber with time of the first fiber module.

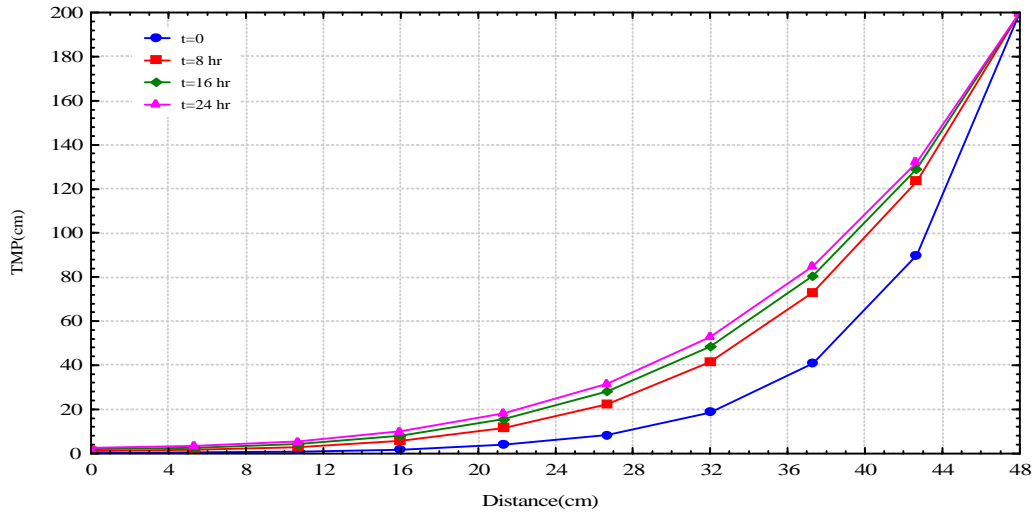


Fig. (7). Variation of TMP along the fiber with time of the first fiber module.

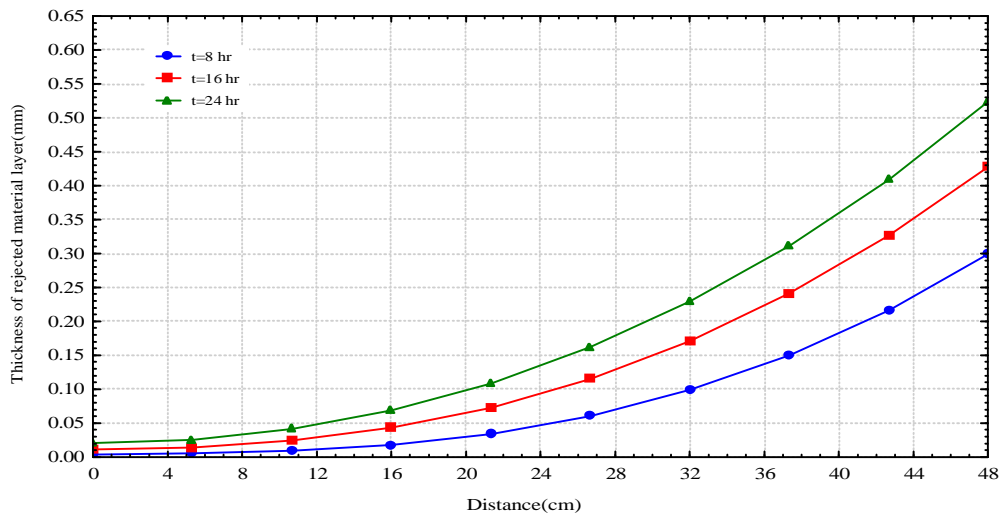


Fig. (8). Variation of the rejected material along the fiber with time of the first fiber module.

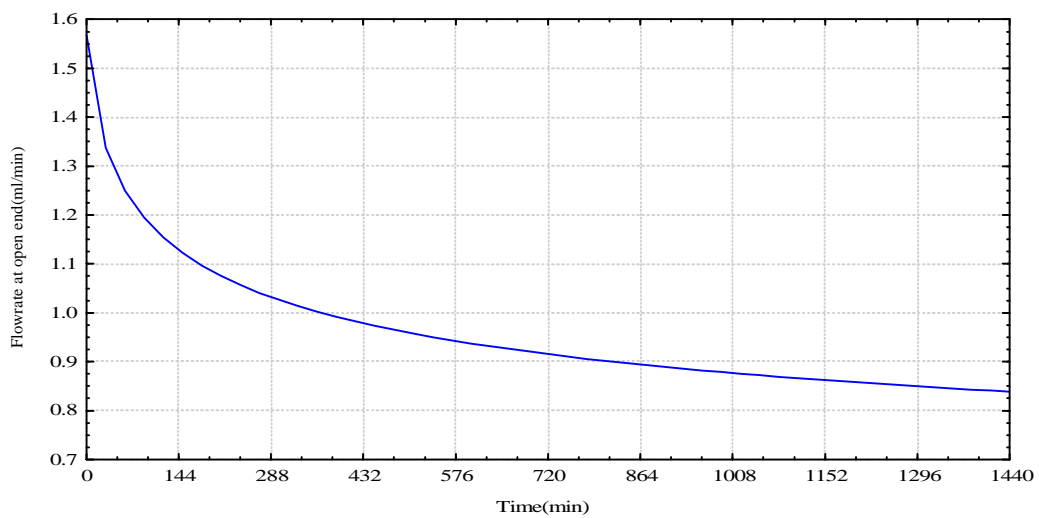


Fig. (9). Variation of the total flowrate with time of the first fiber module.

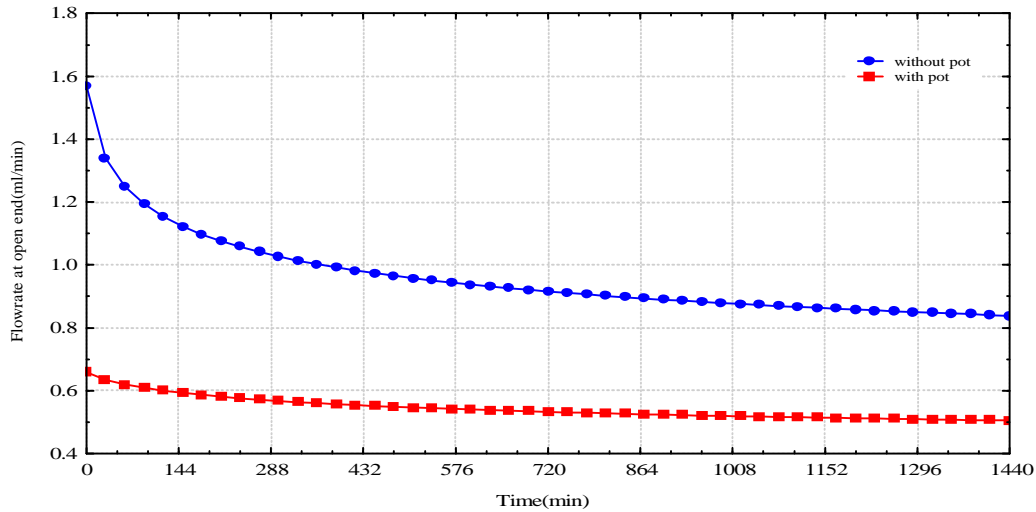


Fig. (10). Effect of pot on the variation of flowrate with time of the first fiber module.

Second Hollow Fiber Membrane Module

The hollow fiber membrane module specifications are listed in **Table (2)**.

Table (2). Specifications of the second hollow fiber membrane module.

Parameter	value
Fiber inner diameter, <i>mm.</i>	0.39
Fiber outer diameter, <i>mm.</i>	0.65
Number of fibers per module.	20 000
Effective fiber length, <i>cm.</i>	100
Pot length, <i>cm.</i>	3.5
Hydraulic conductivity coefficient of membrane, <i>m/sec.</i>	4.64×10^{-9}

Fig.s (11) through (15) show the variation of the flux, transmembrane pressure head, thickness of rejected material layer along the fiber length with time, total fiber flowrate, and the effect of the pot on the ends of the fiber on the total flowrate. Initially, flux follow the same trend of the first type of fiber but the flux drops by 61.5% between the ends of the fiber with less head losses due to the inner diameter is larger then the first type of fibers. The flux drop along the fiber is 48.6% of the t=8hr, dropping to 44.4%, 42.1% for 16 and 24 hrs respectively. The variation of flowrate decline during the first eight hours is about 15.8% down to 7.4% and 4.9% for the second, and last eight hours, respectively. It was found that the flowrate at open end is reduced through the pot length but this decrease change with the time. Initially the decrease is 9.3, dropping to 7.2, 6.6, and 6.2 at t=8, 16, 24 hrs, respectively.

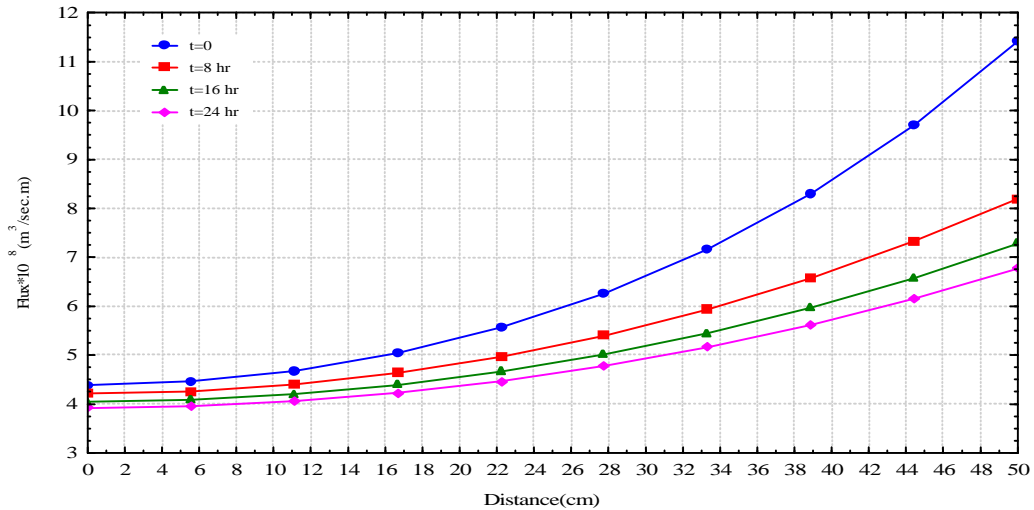


Fig. (11). Flux variation along the fiber with time of second fiber module

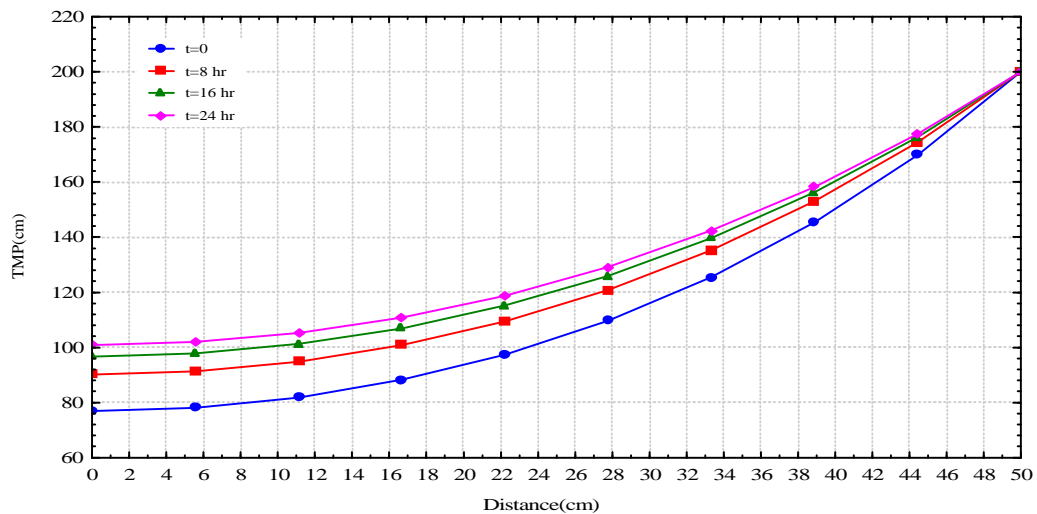


Fig. (12). Variation of TMP along the fiber with time of the second fiber module.

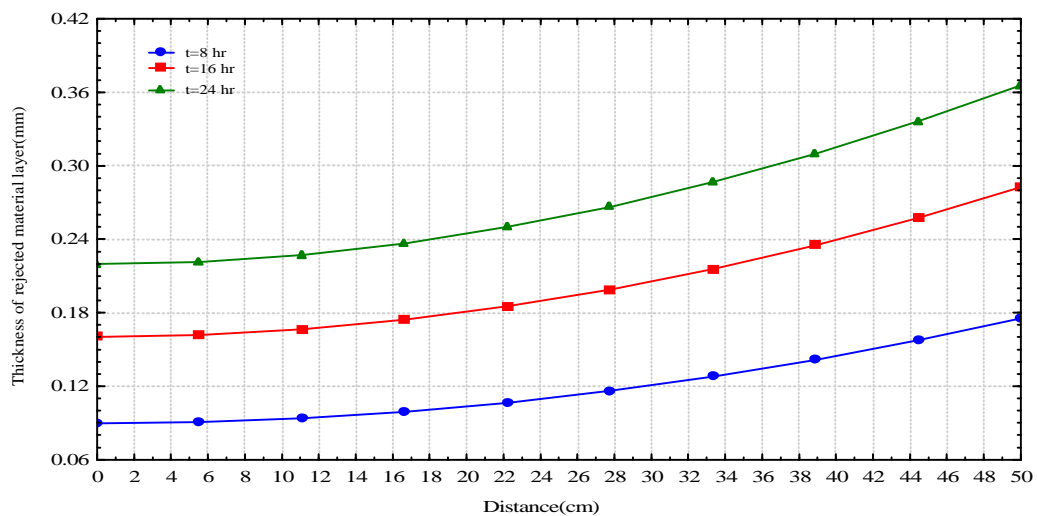


Fig. (13). Variation of the rejected material along the fiber with time of the first fiber module.

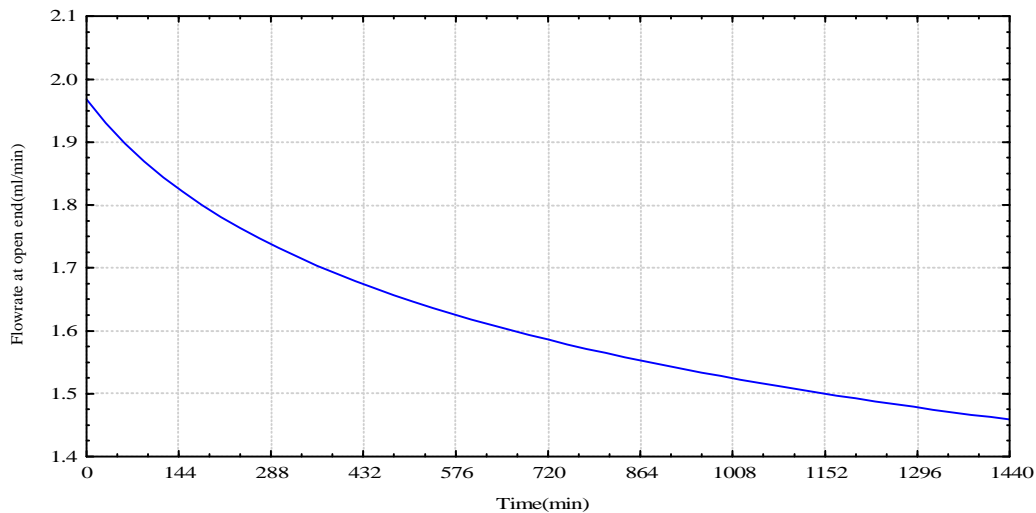


Fig. (14). Variation of the total flowrate with time of the second fiber module.

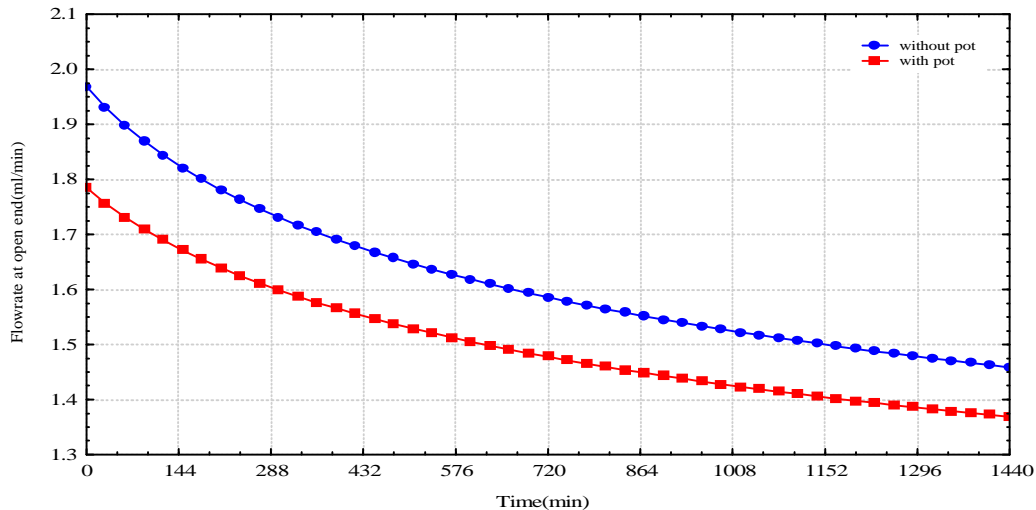


Fig. (15). Effect of pot on the variation of flowrate with time of the second fiber module.

Third Hollow Fiber Membrane Module

The third hollow fiber membrane module specifications are listed in **Table (3)**.

Table (3). Specifications of the third hollow fiber membrane module.

Parameter	value
Fiber inner diameter, <i>mm</i> .	0.8
Fiber outer diameter, <i>mm</i> .	1.20
Effective fiber length, <i>cm</i> .	144.75
Pot length, <i>cm</i> .	4
Membrane hydraulic conductivity coefficient, <i>m/sec</i> .	$2.57 \cdot 10^{-9}$

Figs (16) through (20) show the variation of the flux, transmembrane pressure head, thickness of rejected material layer along the fiber length with time, total fiber flowrate, and the effect of the pot on the ends of the fiber on the total flowrate. The flow follows the same trend of the first and second types of fibers with slight differences reflecting the influence of the large inner diameter of the fiber that reduces the head losses through the fiber channel. Initially, the flux drop is just 9.7% along the fiber, and dropping to 8.4%, 7.7%, and 7.2% after 8, 16, and 24 hrs, respectively. The flowrate decline during the first eight hours is about 7.4%, dropping to 5.2%,

and 4% for the second and last eight hours, respectively. The total flowrate is reduced when using the pot, the Initial decrease is 1%, dropping to 0.93, 0.9, and 0.8 at t=8, 16, 24 hrs, respectively.

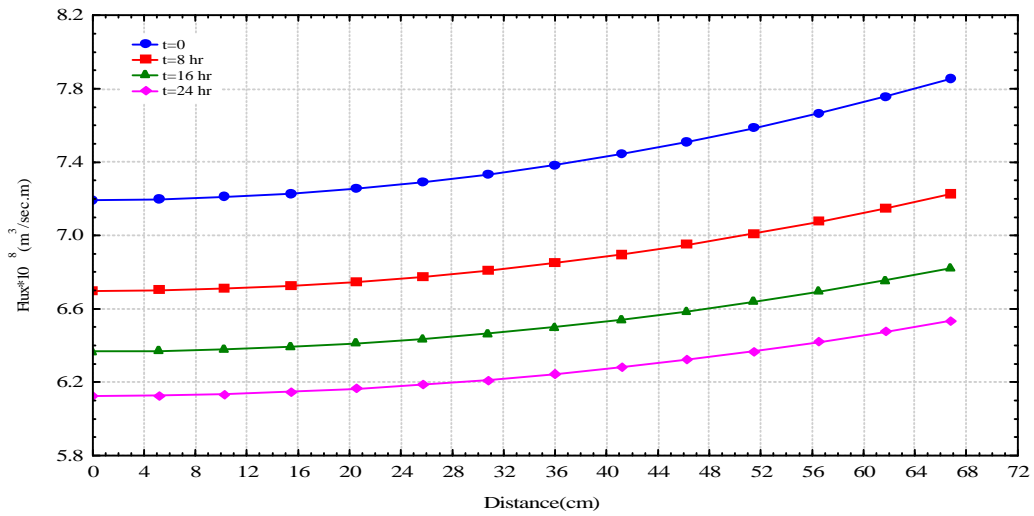


Fig. (16). Flux variation along the fiber with time of third fiber module

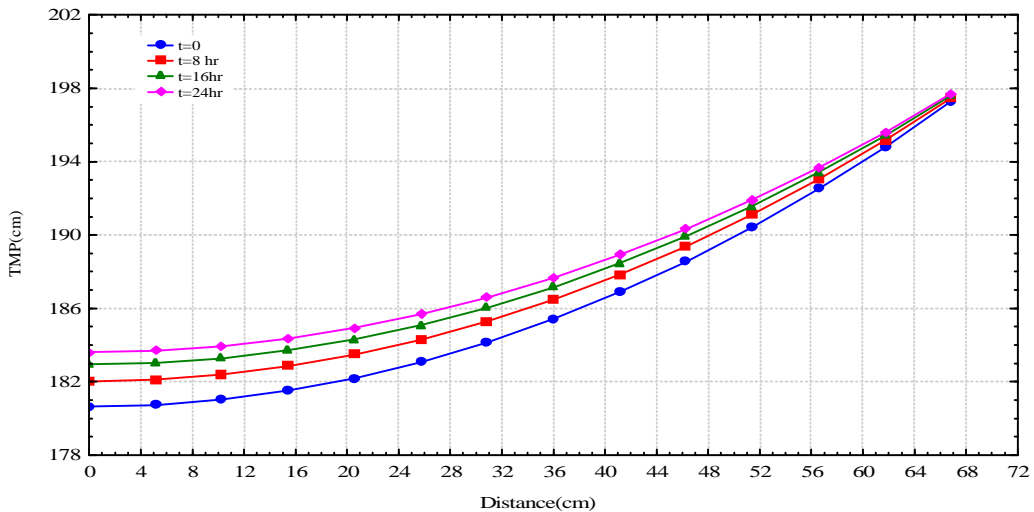


Fig. (17). Variation of TMP along the fiber with time of the third fiber module

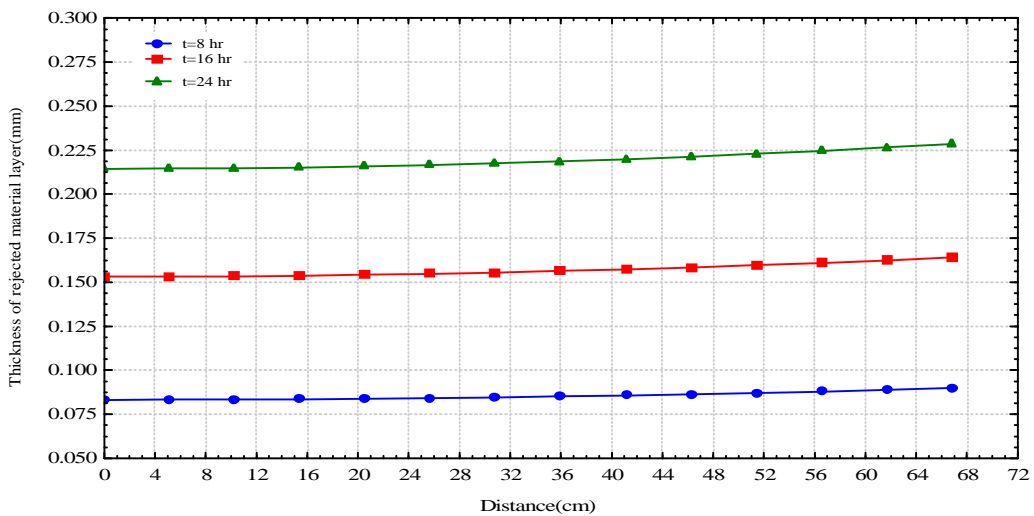


Fig. (18). Variation of the rejected material along the fiber with time of the third fiber module.

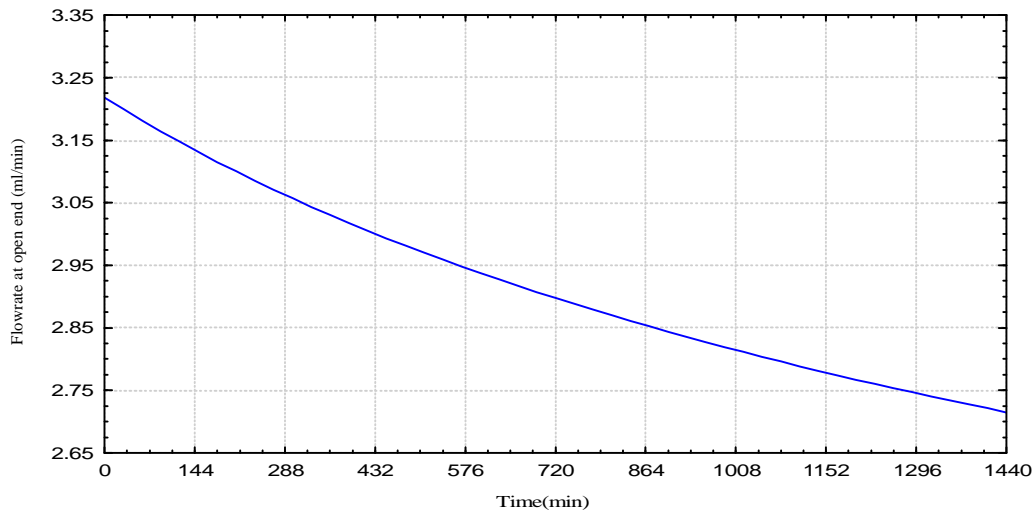


Fig. (19). Variation of the total flowrate with time of the third fiber module.

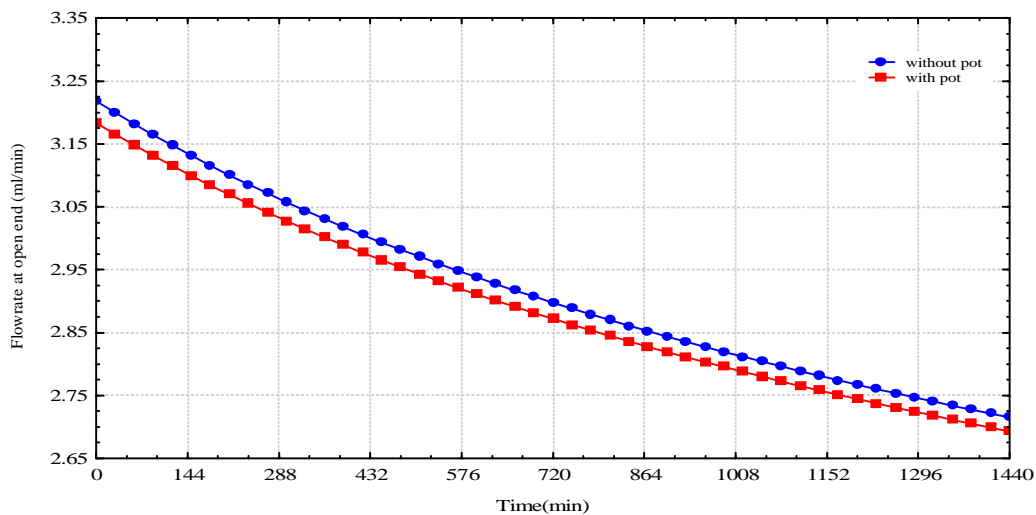


Fig. (20). Effect of pot on the variation of flowrate with time of the third fiber module.

CONCLUSIONS

1. The flow through the hollow fiber membrane under the condition of unsteady flow could be simulated mathematically by applying the equations governing the flow inside the fiber channel, and the fiber wall and equations governing the flow conditions at the boundaries. A very good agreement was found between the laboratory and predicted data under the same conditions.
2. There is a great difference in hydraulic performance of the commercially available hollow fiber membrane and each has its design criteria.
3. The flux is initially nonuniformly distributed along fibers due to the nonuniform distribution of the transmembrane pressure; this fact leads to a nonuniform distribution of the rejected material along the fiber. this nonuniformity increases as the inner fiber diameter decreases.
4. The pot has an effect of reduction the total flowrate. This effect increases as the inner fiber diameter decreases.

5. The thickness of the rejected material on the surface of large inner fiber diameter is of a less thickness than that of small inner diameter for the same amount filtrated water volume, which leads to less flow resistance.

RECOMMENDATIONS

The following recommendations were found to provide a guide for further studies:

1. Study the effect of variation of the applied head with the time under normal operation conditions.
2. Study the optimal design criteria for the hollow fiber membrane.

REFERENCES

- * AL Zubaidy, R. Z. , 2007, Mathematical Simulation of the Flow through Hollow Fibre Membrane under Constant Hydraulic Conductivity, J. Eng., Vol. 13, No. 3.
- * Baker, R. W., 2004, Membrane Technology and Applications, 2nd Edition, John Wiley and Sons Ltd, England.
- * Chaudhary, M. H., 1986, Applied Hydraulic Transients, 2nd Edition, Van Nostrand Reinhold Co., New York.
- * Porter, M. C., 1990, Handbook of Industrial Membrane Technology, Reprint Edition, Noyes publications, United States of America.
- * Singh, A., and Punmia, B. C., 1970, Soil Mechanics and Foundations, Rajinder Kumar Jain.

LIST OF SYMBOLS

α = inclined fiber with the horizontal coordinate.

ρc = particle density, (M/L³).

Θ = Weight factor for variation with respect to t-axis.

Δt = the increment of the time, (T).

Δx = the increment of the distance, (L).

A = cross sectional area of fiber channel, (L²).

a = speed of the pressure wave, (L/T).

A_w = flow sectional area of the fiber wall, (L²).

C = feed water concentration, (M/L³).

C_i = Function identifying equation of continuity.

f = friction factor, (dimensionless).

g = gravitational acceleration, (L/T²).

H = piezometric head, (L).

i = A subscript refers to distance segment sequence; a subscript refers to node number.

i_d = inner diameter of the fiber, (L).

i_w = hydraulic gradient through the fiber wall, (L/L).

j = A superscript refers to time segment sequence.

K = The variable of finite difference expressions conveyance.

K_c = the rejected material hydraulic conductivity, (L/T).

K_{eq} = equivalent hydraulic conductivity, (L/T).

K_f = bulk modulus of elasticity of fluid, (M/L.T²).

K_w = hydraulic conductivity of the fiber wall, (L/T).

L = Half of the effective length fiber, (L).

L_{pot} = The pot distance, (L).

L_{total} = The effective length of fiber, (L).

M_i = Function identifying equation of momentum.

N = Subscript identifying downstream boundary.

Q = flowrate, (L³/T).



qw = flux (lateral inflow rate per unit length of fiber, volumetric flowrate through the fiber wall per unit of fiber length), ($L^3/L.T$).

Q_w = volumetric flux through the fiber wall, (L^3/T).

r = the fiber radius, (L).

r_i = the fiber inner radius, (L).

r_o = the fiber outer radius, (L).

r_{ot} = the rejected material layer outer radius, (L).

t = time, (T).

th = wall thickness, (L).

TMP = Transmembrane pressure head, (H_o-H), (L).

x = horizontal distance along fiber, (L).